Emission of electrons from clean and modified Ru(0001) surfaces by low-energy Na^+ bombardment

J. A. Yarmoff* and H. T. Than
Department of Physics, University of California, Riverside, California 92521

Z. Sroubek
Institute of Radio Engineering and Electronics, Academy of Sciences of Czech Republic, Chaberská 57, 182 51 Prague 8, Czech Republic
(Received 15 January 2002; published 13 May 2002)

Kinetic electron emission (KEE) arising from low-energy (120–1620 eV) Na^+ impact on clean Ru(0001) and Ru(0001) covered with submonolayers of Na, I, Cl, and O is investigated. The observed KEE can be consistently explained by a nonadiabatic electron emission process. As the projectile approaches the surface, electrons in the surface bands are excited by the time variation of the interaction between the projectile and surface. The electron emission mechanism is strongly dependent on the Na^+ impact velocity v and on the surface work function ϕ. The interaction is characterized by γ, the inverse value of the interaction length. It is possible to quantitatively reproduce the dependence of the electron yield on v and ϕ with a single value of γ, even in the presence of adsorbates. For oxygen adsorption and, to a lesser extent, for Cl adsorption, however, the electron energy spectra are broadened. This broadening, tentatively ascribed to electron-electron interactions, has been included in the model and explains the specific features of O/Ru and Cl/Ru quite well. For Cl/Ru and I/Ru, small contributions of a low-energy Auger emission process have also been identified.

DOI: 10.1103/PhysRevB.65.205412 PACS number(s): 73.20.Hb, 34.50.Dy, 79.20.Rf

I. INTRODUCTION

Whereas potential electron emission (PEE) from solid substrates bombarded by ions is understood fairly well,[1] various aspects of kinetic electron emission (KEE) are still a matter of controversy. Direct electron-particle collisions,[2,3] promotion effects,[4] and the recently reported surface-assisted electron emission[5,6] are assumed to all be relevant mechanisms of KEE. It is often difficult to experimentally distinguish between these processes, however. This study involves a detailed analysis of a system for which surface-assisted KEE is the primary mechanism. Ru(0001) is used for this purpose as it is a metal which can be thoroughly cleaned in vacuum, particularly of oxygen which can greatly effect the electron yield. The use of Na^+ as the projectile excludes any PEE because of its small ionization energy of 5.1 eV, thus making the interpretation of electron emission straightforward in terms of some form of KEE.

A topic of both fundamental and practical importance is the strong influence of surface adsorbates on the intensity of KEE. In particular, a large increase in the KEE yield is observed if clean metal surfaces are covered by a submonolayer of oxygen.[7–9] The physical mechanism that leads to such an enhancement has not yet been unambiguously identified. Note that a new process of ion-induced electron emission from metal-oxygen bonds has been suggested as a possible source of the intense KEE from oxidized surfaces.[10] In contrast, however, the analysis in this paper does not introduce any new mechanisms to describe electron emission in the presence of adsorbates.

The experimental data collected from Ru covered by Na, I, Cl, and O are interpreted within the same conceptual framework as for clean Ru. The only parameter employed in the analysis is the inverse value of the particle-surface interaction distance, which is denoted by γ.[5,6] In this approach, the value of γ is deduced by fitting experimental data to the model. In order to provide a strong physical justification for the model, the data are fit using a minimal number of adjustable parameters. The key parameter γ is kept the same for all surface compositions, and the effects due to adsorbates are described only by changes of the work function ϕ. Because the work function is measured by independent means, ϕ is not itself a new parameter. For clean Ru and for Ru with small Na and I coverages, the data are reproduced by the model to within better than a factor of 2. This is in spite of the fact that the yield changes by almost 4 orders of magnitude over the range of ion energies employed. However, for Cl and particularly for O, the measured yields differ considerably from the predictions based on the model in which only ϕ is changed. The spectra themselves indicate that the electron distributions for O/Ru and Cl/Ru are slightly broader. If a correction for broadening is included explicitly in the model, the fitting of the O/Ru and Cl/Ru data can again be made nearly perfect. The degree of the broadening, its physical origin, and its justification are discussed below.

II. EXPERIMENTAL PROCEDURE

The experiments were performed in an ultrahigh-vacuum (UHV) chamber that has a base pressure below 10^{-10} Torr. The chamber is equipped with a cylindrical mirror analyzer (Perkin-Elmer) for Auger electron spectroscopy (AES), low-energy electron diffraction (LEED) optics (Princeton), and a low-energy electron gun, which is used to generate secondaries for work function measurements. An alkali ion gun (Kimball Physics) mounted on a rotatable turntable was used to produce the Na^+ ions for these experiments. The emitted electrons were collected by a Comstock electrostatic analyzer (ESA) mounted in the same plane as the electron and alkali ion guns. The ESA employs double-focusing 160°

spherical sectors and contains an Einzel lens at the entrance for focusing.

The details of the sample cleaning procedure are described elsewhere.[11] Briefly, the Ru(0001) crystal was cleaned with several cycles of 1-keV Ar^+ bombardment and annealing at 1400 K. The sample was further cleaned by heating in 10^{-7} Torr of O_2 at 1100 K, which removes C and S. Prior to each measurement, a final anneal was performed for 1 min at 1600 K. During the final heating, the base pressure did not exceed 5×10^{-10} Torr.

The cleanliness and ordering of the surface were checked with AES and LEED. After the cleaning procedure was complete, AES showed no detectable contamination and a sharp (1×1) LEED pattern was obtained. It is difficult, however, to ensure that the surface is completely free of C and S, which are the major impurities, because the C and Ru AES lines overlap. To overcome this difficulty, the peak ratios of the AES Ru_+/Ru_- at 273 and 150 eV were monitored, as described in Ref. 12.

Iodine and chlorine were deposited from solid-state electrochemical cells, which are based on Ag halide pellets.[13] For Na deposition, a well-outgassed dispenser source (SAES getter) was used. During halogen and Na deposition, the pressure did not exceed 2×10^{-10} Torr. Oxygen was deposited by backfilling the chamber with O_2 through a sapphire leak-valve.

The Na^+ ion beam was incident onto the sample at an angle of 15° with respect to the surface normal. Negative particles produced by the ion impact were collected by the ESA at normal emission. In order to reduce the effect of stray magnetic fields, a bias of -20 V was applied to the sample. This accelerates the electrons with zero kinetic energy—i.e., those right at the vacuum level of the sample—to 20 eV. This energy is sufficiently high that the electrons are unaffected by the stray fields, as determined empirically. Because of the bias voltage, all of the cutoffs in the figures occur at approximately 20 eV. The work function of the clean surface was taken from the literature to be 5.3 eV.[14] Movements of the electron cutoff position were used to determine the work function changes that occurred as the surface was modified by adsorption. Examples of the measured energy distributions for different Na^+ projectile energies are shown by symbols for different adsorbates in Fig. 1 (clean Ru), Fig. 3 (I/Ru), Fig. 5 (Cl/Ru), and Fig. 7 (O/Ru).

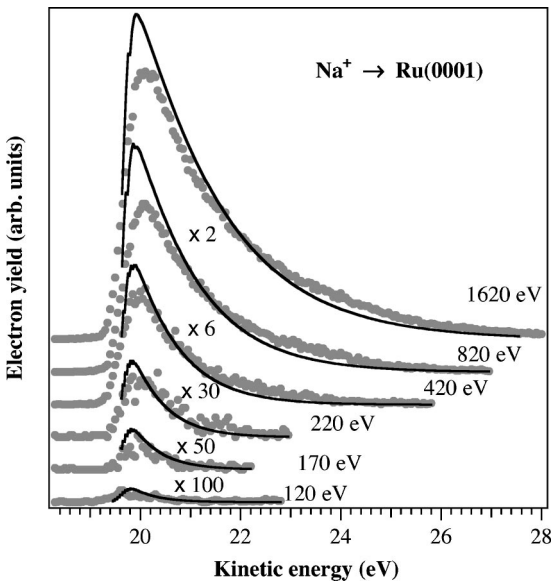

FIG. 1. Kinetic energy distributions of electrons emitted during bombardment of clean Ru(0001) by Na^+ ions of the indicated energy. The solid circles show the raw experimental data, while the solid lines show calculated results (see text). The sample was biased at -20 V, so the secondary-electron cutoff appears near 20 eV. The spectra are offset from each other for display purposes.

III. DESCRIPTION OF THE MODEL AND ANALYSIS OF THE DATA

A. Clean Ru(0001)

Figure 1 shows the data collected from clean Ru(0001) for various Na^+ incident energies. The gray dots show the raw experimental data, while the solid line shows a theoretical fit to the data, which is discussed below. When the incident ion energy is increased, the electron yield increases and the distributions broaden, while the positions of the cutoffs are unchanged.

The mechanism proposed for the observed electron emission is the surface-assisted KEE process that was identified for Al bombarded by Li^+ Ref. 5 and for other systems.[6] The model is based on the fact that the interaction of the impinging particle with the substrate changes rapidly with time as the particle approaches the surface. In Ref. 5 the relevant part of the interaction was assumed to be due to electron transfer from the localized orbital of the projectile to the continuum of states of the solid. Such an approach allows the magnitude of the interaction to be deduced from charge exchange experiments, particularly from data on ion scattering.[15] However, in many systems this may not be the only process leading to electron excitation and the direct interaction of the particle potential with solid-state electrons must also be taken into account. Currently, there is no theoretical expression available to describe this general interaction, however, so we have to resort to semiempirical estimates. Inside the solid the interaction of the particle with electrons leads to the well-known stopping power,[16,17] while outside the sample the stopping power is zero. Thus we may schematically model the matrix element of the potential between the particle and the electron states of the solid by

$$V(t)=Ve^{2\gamma v t} \quad \text{for } 0>t>-\infty,$$

$$V(t)=V \quad \text{for } t>0, \tag{1}$$

where γ is the inverse value of the interaction distance from the surface, v is the perpendicular component of the velocity of the bombarding particle, and $t=0$ is the impact time. The change of $V(t)$ at $t=0$ (i.e., at the surface) must be smooth in real systems, which is not the case in the simplified schematic expressions (1). The value of V can be approximately adjusted by fitting V to the stopping power of the particle in the solid.[17] In Eqs. (1) the matrix element is constant for $t>0$, while in reality it changes in time with the periodicity

of the electron wave functions in the solid. It should be stressed that excitation and emission are basically many-electron processes and are described by Eqs. (1) only schematically.

The Fourier transform of a properly smoothed $|V(t)|^2$ leads to the following physically appealing approximate form for the energy distribution $f(\varepsilon)$ of electrons excited to energies ε above the Fermi energy ε_F of the solid[6] [note that atomic units (a.u.) are used throughout this paper]:

$$f(\varepsilon)=\frac{A}{\gamma v}\frac{1}{\exp\left(\frac{\pi}{2\gamma v}(\varepsilon-\varepsilon_F)\right)+1}. \tag{2}$$

Note that A contains the square of V. In actual experiments, however, the value of A cannot be easily deduced because this would require a precise knowledge of the collection efficiency of the apparatus. Thus A has a rather arbitrary value, but this value is kept fixed in analyzing all of the data collected. Of particular interest in our analysis is the value of γ, which can be deduced rather precisely by fitting Eq. (2) to the experimental data. Because the value of γ determines the width of the energy distribution of the emitted electrons, it also very strongly influences the intensity of electron emission, particularly for substrates with large work functions. The value of γ turns out to be consistently larger, especially for heavier projectiles, than would be expected from a one-electron theory. The discrepancy may be due to the neglected role of inner, more spatially confined electron orbitals or possibly due to other, not-yet-determined many-electron processes. The way that γ of a given substrate is influenced by the adsorbates and by the bombarding particle is thus of special interest.

The exponent in Eq. (2) in this case is always negative and substantially larger than 1. Thus Eq. (2) can be rewritten as

$$f(E)=\frac{A}{\gamma v}\exp\left(-\frac{\pi}{2\gamma v}(E+\phi)\right), \tag{3}$$

where $E=\varepsilon-\varepsilon_F-\phi$, and ϕ is the work function of the solid. This is a more convenient form for comparison to experiment.

The actual measured kinetic energy distributions, however, are deformed by the refraction of electrons at the surface barrier and by the energy-dependent transport of electrons from the sample to the entrance of the ESA. We will now discuss modifications of $f(E)$ that can be used to account for these effects.

The surface refraction can be easily taken into account if we assume that the angular distribution of electrons is isotropic inside the solid. In the configuration employed, the detected electrons are those emitted normal to the surface in a very narrow angle. Then, according to Ref. 18, the distribution of emitted electrons inside the solid, given by Eq. (3), must be multiplied by a function $D(E)$, which is equal to

$$D(E)=\frac{E}{E+\phi}. \tag{4}$$

The transfer of electrons from the sample to the entrance of the ESA spectrometer would be energy independent if the space between the sample and spectrometer were field free. However, we used a negative bias u on the sample in order to increase the sensitivity and to suppress the effects of stray magnetic fields. Another consequence of the field is that the emitted electrons are accelerated so that the lowest-energy electrons are preferentially focused into the spectrometer and their intensity is effectively enhanced. The transfer can be easily modeled, however, if we assume a slightly simplified configuration of the sample and of the entrance to the ESA. The sample is represented by an infinite plane separated from the ESA by the distance l and set at the potential u with respect to the spectrometer. The spectrometer is represented by an infinite plane with an opening of the radius d. If $d \ll l$, it can be shown that the number of detected electrons remaining from a total of N electrons emitted isotropically from the sample in front of the opening is equal to

$$N\frac{1}{2}\left(\frac{d}{l}\right)^2 T(E,u)=\frac{N}{2}\left(\frac{d}{l}\right)^2\left(\frac{u}{2E}\right)^2\left(\sqrt{1+\frac{u}{E}}-1\right)^{-2}, \tag{5}$$

where $1/2\ (d/l)^2$ is the relative fraction of detected electrons when the bias voltage u is equal to zero [for a given experimental setup, it is a constant that is included in the preexponential factor A in Eq. (3)], and $T(E,u)$ is the energy-dependent transfer function. $T(E,u)$, as given by Eq. (5), is invalid for very small E. For example, for $u=20$ V, it is not correct for about $E<0.5$ eV (it is constant rather than proportional to E^{-1} below 0.5 eV).

After these corrections are taken into account, the number of detected electrons, $n(E)$, within the energy interval E and $E+dE$, i.e., the energy spectrum, would be given by

$$n(E)=f(E)D(E)T(E,u). \tag{6}$$

However, to directly compare calculated energy spectra with the measured ones, we still need to take into account the broadening due to the finite resolution of the ESA. To do so, we convolute $n(E)$ with the normalized convolution function

$$R(E')=\frac{1}{\sqrt{\pi}\,\Delta E}\exp\left(-\frac{(E-E')^2}{(\Delta E)^2}\right), \tag{7}$$

where ΔE is the bandpass energy width of the ESA, which is a known quantity. The calculated spectra that are shown in this paper were thus obtained by convolution of Eq. (6) with Eq. (7).

It also useful to study the total number of emitted electrons, Γ, as a function of the impact particle velocity and adsorbate coverage. Γ is given by the integral

$$\Gamma=\int_0^\infty n(E)dE. \tag{8}$$

It should be noted that for electron energies E smaller than the bias u and the work function ϕ, the function $D(E)$ is proportional to E and $T(E,u)$ is proportional to E^{-1}, so that

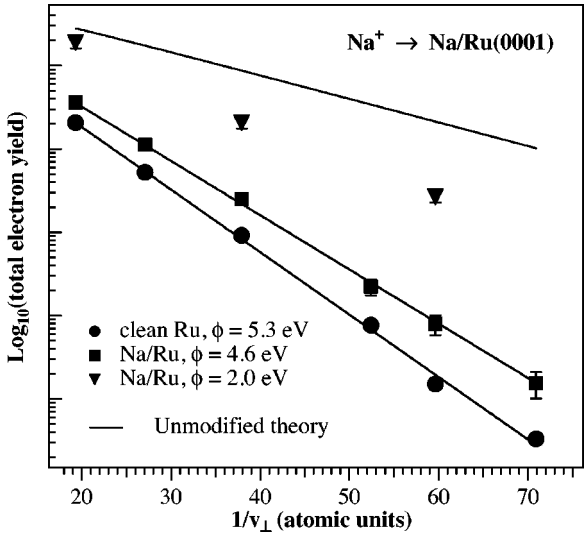

FIG. 2. Total yield of electrons emitted from clean and Na-covered Ru(0001) plotted as a function of the inverse of the perpendicular component of the velocity of the incident Na^+ ions. The symbols show the experimental data, while the solid lines show the expected behavior based upon the nonadiabatic model assuming the indicated work function values.

the product $D(E)T(E,u)$ is independent of E and very close to 1. In this approximation, we obtain from Eqs. (3) and (9) that

$$\Gamma = \frac{2A}{\pi}\exp\left(-\frac{\pi}{2\gamma v}\phi\right). \tag{9}$$

The physically interesting parameters in the energy distribution function $f(E)$ of electrons emitted from clean Ru surfaces can be deduced directly from comparison of the measured energy distributions $n(E)$ in Fig. 1 with Eq. (6). The analysis is simpler, however, if we first compare the integrated electron yield Γ, rather than $n(E)$, with the theoretical predictions.

The measured Γ's were obtained from the energy distributions $n(E)$, such as those shown by the gray dots in Fig. 1, via numerical integration, according to Eq. (8). These experimental Γ's are shown as a function of $1/v$ for clean Ru(0001) by the solid circles (●) in Fig. 2. The calculated values of Γ are determined by integration of Eq. (6) and are shown as solid lines in Fig. 2. Using a work function of $\phi = 5.3$ eV for clean Ru, the best fit of the model with experiment is obtained with $\gamma = 1.8$ (in a.u.) and $A = 1650$. It is obvious from this semilogarithmic plot that Γ depends exponentially on $1/v$ in the whole range of the Na^+ primary energies used here. Note that the extreme values of $1/v$ are equal to 73 and 18.3 (in a.u.), which correspond to incident Na^+ kinetic energies of 100 and 1600 eV, respectively. As discussed above, the total yield Γ can also be well approximated by a simple analytical expression given by Eq. (9). This approximate yield also depends exponentially on $1/v$, and we can deduce the value of γ with sufficient precision by comparing the experimental data to Eq. (9), as well. It should be noted that Γ in Fig. 2 does not show any deviation from linearity at small v; thus, any "hot spots," such as those noticed for heavy projectiles in Ref. 6, are absent here. The constant A, as has already been mentioned, includes the experimental collection efficiency. In this sense, it has an arbitrary value, but this value should be the same for all of the experiments performed with this apparatus. Therefore, a value of $A = 1650$ is used throughout this study.

TABLE I. Parameters used to interpret the experimental data (see text).

System	Work function ϕ (eV)	γ (a.u.)	k
Clean Ru	5.3	1.8	1
Ru+Na	5.1–2.0	1.8	1
Cl/Ru	5.7	1.8	1
I/Ru	4.6	1.8	1
O/Ru (0.1 ML)	5.7	1.8	1.32
O/Ru (0.3 ML)	6.2	1.8	1.60

To test the consistency of the model, we also calculated the electron energy distribution $n(E)$ using Eqs. (3), (6), and (7) and the same parameters $\gamma = 1.8$ and $A = 1650$. The calculated $n(E)$ are shown for different impact energies by solid lines in Fig. 1. The theoretical and experimental $n(E)$ are very close to each other, despite the fact that the number of emitted electrons changes by several orders of magnitude as the incident energy is varied. Such good agreement attests to the consistency and validity of the model employed here. The values of the parameters used to interpret the data collected from clean and adsorbate-covered Ru(0001) are all summarized in Table I.

B. Na/Ru(0001)

In the next experiment, a small amount of Na was deposited on the Ru surface, which lowered the work function to $\phi = 4.6$ eV. This work function change implies a surface coverage of about 0.03 monolayers (ML).[19] The corresponding experimental values of Γ are shown by solid squares (■) in Fig. 2 as a function of $1/v$. The calculated Γ, again with $\gamma = 1.8$ and $A = 1650$, is shown by a line in Fig. 2. The line matches the experimental data rather well and reproduces not only the slope, but also the increase in intensity from that of clean Ru.

Also shown in Fig. 2 are the total yield experimental data [solid triangles (▼)] and the theoretical predictions (the line near the top of the figure) for a larger Na coverage. For this sample, the work function was lowered to $\phi = 2.0$ eV, which implies a coverage of at least 0.25 ML.[19] The agreement between the theory and experiment is less satisfying in this case, however, as the theory predicts more emission than is actually observed, particularly at low impact energies. We do not know if this disagreement points to some fundamental flaw in the model or if it is due to physical conditions on the surface of Ru covered by a large amount of Na. For example, at these coverages Na may form heterogeneous islands so that there are large patches with different work functions across the sample surface. The cutoff used to measure ϕ actually represents the value of the region with the lowest

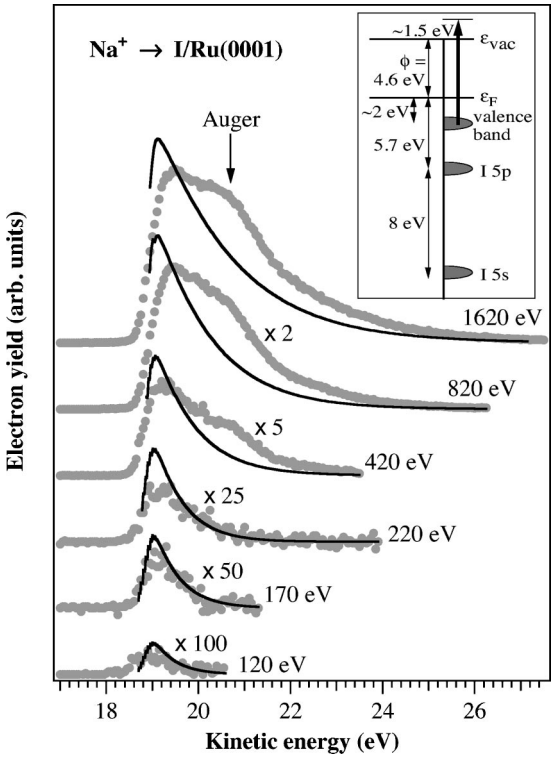

FIG. 3. Kinetic energy distributions of electrons emitted during bombardment of iodine-covered Ru(0001) by Na^+ ions of the indicated kinetic energy. The solid circles show the raw experimental data, while the solid lines show calculated results (see text). The spectra are offset from each other for display purposes. The inset shows a schematic diagram of the energy levels involved in the production of the Auger feature.

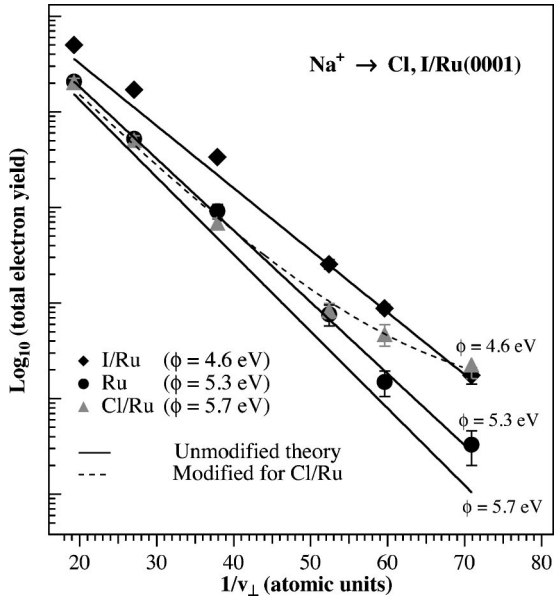

FIG. 4. Total yield of electrons emitted from clean and I- and Cl-covered Ru(0001) plotted as a function of the inverse of the perpendicular component of the velocity of the incident Na^+ ions. The symbols show the experimental data, while the solid lines show the expected behavior based upon the nonadiabatic model assuming the indicated work function values. The dashed line shows the results of a modification of the theory applied to the Cl-covered surface (see text).

work function, and the theory is based on this number. Thus the average work function of the sample may actually be larger than 2.0 eV, so that the measured yield is reduced from that predicted.

C. I/Ru(0001)

Figure 3 shows electron kinetic energy distributions collected from I-covered Ru(0001). The adsorption of iodine lowered to work function to 4.6 eV, which is the same value as the low-coverage Na-adsorbed surface discussed above. As with clean Ru, the yield increases as the incident ion energy is raised. In this case, however, the spectral shape changes dramatically with incident energy, as there is an extra feature apparent, particularly in the high-impact-energy spectra.

This new feature, which is located about 2 eV above the cutoff, is presumably due to low-energy Auger transitions associated with the iodine adsorbate. The most likely scenario for the production of such an Auger feature is that a hole is initially created in the $5s$ state of iodine. The hole in the I $5s$ state can then be filled by an electron from the I $5p$ state, while a second electron is emitted by an Auger process from occupied states just below the Fermi energy ε_F. The data of Ref. 20 indicate that the I $5s$ state is located about 8 eV below the I $5p$ state. The peak in the density of filled states for Ru occurs at about 2 eV below ε_F.[21] If it is thus assumed that most of the electrons are emitted from about 2 eV below ε_F and because the work function of I/Ru is 4.6 eV, the Auger electron yield would peak at about 1.4 eV above the cutoff, which is consistent with what is experimentally observed. Note that we can exclude a scheme in which a hole is initially created in the I $5p$ level and filled by electrons from below the Fermi level, since the $5p$ binding energy is only 5.7 eV.[20] The relevant energy levels for this process are shown in the inset to Fig. 3.

The fact that the feature is observed only at the highest incident ion energies is consistent with the notion that there is a minimum amount of ion kinetic energy required to produce the energy level promotion and to create the hole from which the Auger decay is initiated. It is not impossible, however, that the holes are created by ion-induced secondary electrons rather than by ion-induced level promotion. In fact, the I $5s$ states are, according to the Fano-Lichten diagrams, not promoted in ion collisions and thus direct hole creation by an energetic electron impact is more likely.

Also shown in Fig. 3 are the theoretical predictions of $n(E)$ obtained from Eqs. (6) and (7). It is seen that the general behavior of the yield is correctly predicted, but in this case the Auger feature alters the shape of the distribution so that the agreement is not nearly as good as for clean Ru(0001) in Fig. 1.

Because of the presence of the Auger feature, a test of the quantitative agreement between experiment and theory can be better achieved by comparing the total integrated yields Γ. In Fig. 4, total yields are shown for the clean surface (same

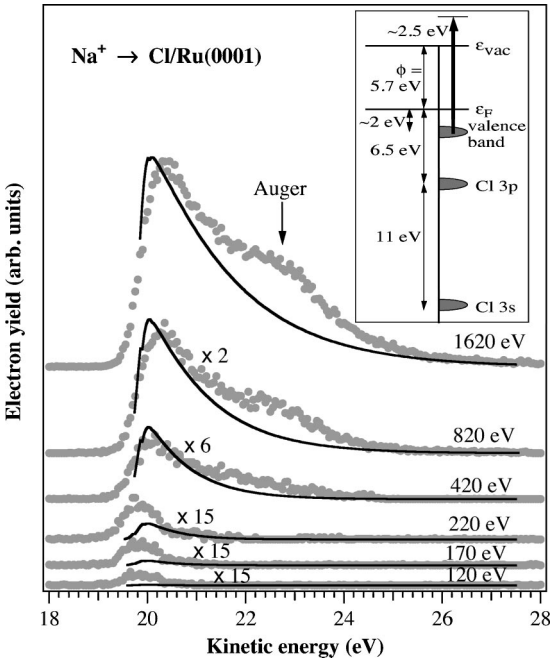

FIG. 5. Kinetic energy distributions of electrons emitted during bombardment of chlorine-covered Ru(0001) by Na^+ ions of the indicated kinetic energy. The solid circles show the raw experimental data, while the solid lines show calculated results (see text). The spectra are offset from each other for display purposes. The inset shows a schematic diagram of the energy levels involved in the production of the Auger feature.

data as in Fig. 2) and for the iodine- and chlorine- (discussed below) covered surfaces. The solid diamonds (◆) show the experimentally determined values of Γ as a function of $1/v$ for Ru covered by iodine. The values of Γ were obtained by integration of the $n(E)$ shown in Fig. 3. The theoretical Γ, with $\gamma=1.8$, $A=1650$, and $\phi=4.6$ eV, are indicated in Fig. 4 by a solid line. The theoretical prediction is in good agreement with experiment, except at high impact energies where the measured yield is slightly higher. This slight deviation is presumably due to the contribution of the Auger feature to the total yield.

D. Cl/Ru

Chlorine adsorption raised the surface work function to 5.7 eV. The electron kinetic energy distributions collected from the Cl-covered surface are shown in Fig. 5. Also shown in Fig. 5 are the theoretical predictions based on Eqs. (6) and (7). Similar to I/Ru, the shapes of the experimental spectra are obscured by a peak, located at about 3 eV above the cutoff, which also becomes prominent at the highest Na^+ impact energies. This is again likely due to an Auger process.

The Auger feature may have the same explanation as in the case of iodine. The likely mechanism is the filling of a Cl $3s$ hole with an electron from the Cl $3p$ level. Ultraviolet photoemission spectroscopy (UPS) spectra collected from Cl adsorbed onto Ru (Ref. 21) show a peak at about 6.5 eV, which is presumably related to the Cl $3p$ level. The UPS spectra of $CrCl_3$ and $RuCl_3$ (Ref. 22) show that the Cl $3p$ and Cl $3s$ features are separated by about 10–11 eV. If it is assumed, as was done for I/Ru, that most of the electrons are emitted from 2 eV below ε_F and because the work function of Cl/Ru is 5.7 eV, the Auger electrons would then have a kinetic energy of ~3 eV, which is in agreement with the experimental results. The relevant energy levels of Cl/Ru are shown in the inset to Fig. 5.

The integrated measured intensity of electrons emitted from Ru covered by Cl is shown in Fig. 4 by the solid triangles (▲). The calculated Γ with $\gamma=1.8$, $A=1650$, and $\phi=5.7$ eV is shown in the same figure as a function of $1/v$ by a solid line that is nearly straight. In this case, however, the experimental yield does not follow the straight line, which indicates that it does not depend exponentially on $1/v$ over the whole range of Na^+ primary energies used. The deviation from the theoretical predictions is most pronounced at low impact velocities where the contribution of the Auger process is negligible.

A possible source of the discrepancy at low energy is a broadening of the distribution due to shortening of the lifetime of the electronic states in the substrate. It can be shown that if the lifetime of the electronic states in the substrate is τ, then Eq. (3) can be written in a more general form as

$$f(E)=\frac{A\tau^2}{\gamma v\left(\tau-\frac{\pi}{2\gamma v}\right)}\left(\frac{e^{(-\pi/2\gamma v)(E+\phi)}}{\tau+\frac{\pi}{2\gamma v}}-\frac{1}{2\tau}e^{-\tau(E+\phi)}\right). \tag{10}$$

For $\tau\to\infty$, Eq. (10) becomes equal to Eq. (3). Using Eq. (10) to determine the total yield of emitted electrons, it can be shown that

$$\Gamma=\frac{2A}{\pi}\frac{\tau^2}{\tau^2-\left(\frac{\pi}{2\gamma v}\right)^2}e^{(-\pi/2\gamma v)\phi}-\frac{A}{2\gamma v\left(\tau-\frac{\pi}{2\gamma v}\right)}e^{-\tau\phi}, \tag{11}$$

where the same approximation is used as for Eq. (9), i.e., $D(E)T(E,u)=1$. The resulting theoretical Γ, calculated from Eq. (11) with the standard parameters of $\gamma=1.8$, $A=1650$, and $\phi=5.7$ eV and by setting the broadening $\tau=54.4$ (in a.u.), is shown as a function of $1/v$ in Fig. 4 by the dashed line. The agreement with the experimental data is now very good over the whole range of impact energies. The value of $\tau=54.4$ corresponds to a level broadening with a half-width of about 0.5 eV.

E. O/Ru(0001)

In Fig. 6, solid triangles (▲, ▼) show the total measured electron yields, obtained by integrating the $n(E)$ spectra, as a function of $1/v$ for oxygen coverages of 0.3 and 0.5 ML. For comparison, the $1/v$ dependence of the total yield for clean Ru(0001) is also shown [as solid circles (●)] in the figure. The work function increases with adsorbed oxygen and was measured to be 5.7 and 6.2 eV for the two coverages, respectively. Because the surface work function increases, one would expect a decrease of the electron yield. In contrast, however, the electron yield increases significantly with oxy-

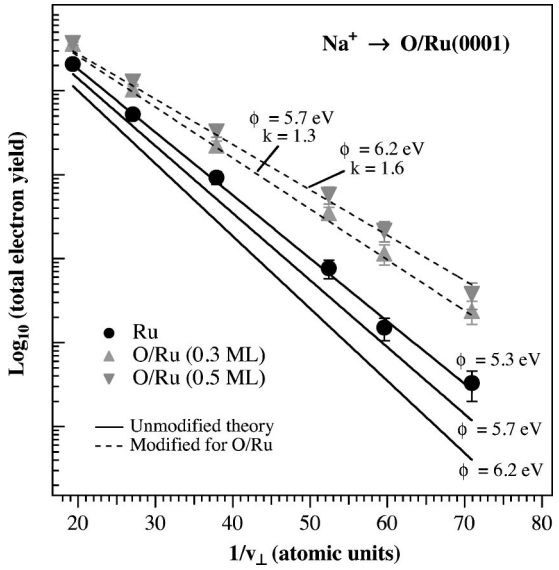

FIG. 6. Total yield of electrons emitted from clean and oxygen-covered Ru(0001) plotted as a function of the inverse of the perpendicular component of the velocity of the incident Na^+ ions. The solid circles (●) show the experimental data collected from clean Ru(0001), while the solid triangles show the experimental data for Ru with 0.3 ML (▲) and 0.5 ML (▼) of adsorbed oxygen. The solid lines show the expected behavior based upon Eq. (9) assuming the indicated work function values. The thicker lines show the expected behavior when broadening due to electron-electron interactions is included in the model by fitting with Eq. (15).

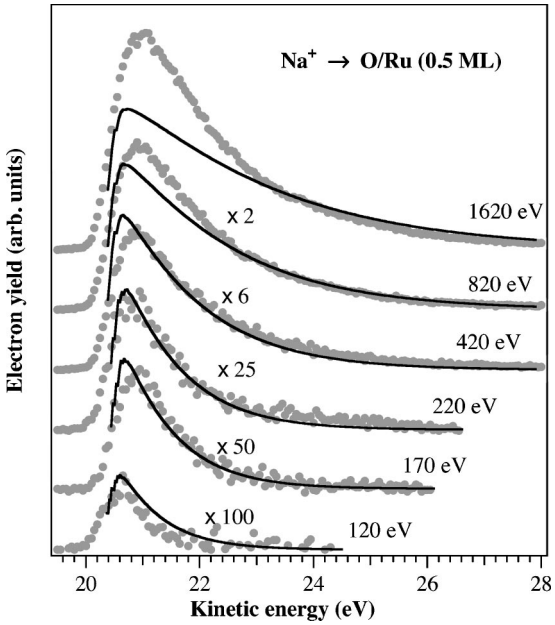

FIG. 7. Kinetic energy distributions of electrons emitted during bombardment of the 0.5 ML oxygen-covered Ru(0001) surface by Na^+ ions of the indicated kinetic energy. The solid circles show the raw experimental data, while the solid lines show calculated results (see text). The spectra are offset from each other for display purposes.

gen adsorption, as can be seen directly by the experimental data shown in the figure. By keeping $\gamma=1.8$ and $A=1650$, the total calculated yields, which are plotted as solid lines in Fig. 6, are indeed much lower than for the clean surface, as is expected from the unmodified theory. The discrepancy between the calculated and the measured dependence is of several orders of magnitude at lower impact velocities.

Adsorbed oxygen ions provide three times more multielectron semilocalized configurations within a few eV from the ground state, as compared to chlorine ions. Thus oxygen may not only decrease the lifetime τ of one-electron states, as assumed in the case of Cl/Ru, but can also broaden the energy distribution of excited electrons by many-electron processes. To allow for such a broadening of the distribution, it is assumed that the form of the distribution would be similar to that given by Eq. (3) for the clean surface, but with γ multiplied by a coefficient k, which is greater than 1, and with a different preexponential factor B instead of A. If the cause of the broadening is electron-electron interactions, we may further assume that the energy deposited in the process would be independent of the broadening and thus independent of k. This assumption would determine the preexponential factor B of the new distribution in terms of A. Using the expression for the deposited energy ΔE,

$$\Delta E(\text{deposited}) = 2\int_{\varepsilon_F}^{\infty} f(\varepsilon-\varepsilon_F)(\varepsilon-\varepsilon_F)d\varepsilon. \qquad (12)$$

The assumed independence of ΔE (deposited) on k gives

$$\int_{\varepsilon_F}^{\infty} \frac{A}{\gamma v} e^{-\pi(\varepsilon-\varepsilon_F)/2\gamma v}(\varepsilon-\varepsilon_F)d\varepsilon = \int_{\varepsilon_F}^{\infty} \frac{B}{k\gamma v} e^{-\pi(\varepsilon-\varepsilon_F)/2k\gamma v}(\varepsilon-\varepsilon_F)d\varepsilon. \qquad (13)$$

From Eq. (13) we obtain the relationship between the preexponential factors A and B as $B=A/k$. The generalized expression for $f(E)$ is then given by

$$f(E) = \frac{A}{k^2\gamma v}\exp\left[-\frac{\pi}{2k\gamma v}(E+\phi)\right]. \qquad (14)$$

The approximate expression for the total yield, analogous to Eq. (9), can then be shown to be

$$\Gamma = \frac{2A}{\pi k}\exp\left(-\frac{\pi}{2k\gamma v}\phi\right). \qquad (15)$$

Note that a value of $k=1$ reduces Eqs. (14) and (15) to Eqs. (3) and (9), respectively.

Relations (14) and (15), with $k>1$, can be used to interpret the data collected from O/Ru quantitatively. If we take $k=1.32$ for 0.3 ML and $k=1.60$ for for 0.5 ML (keeping $A=1650$ and $\gamma=1.8$, as for clean Ru), we can fit the experimental total electron yields rather well, as seen in Fig. 6. The dashed lines, representing the calculated dependences, pass directly through the experimental points at lower impact energies (high $1/v$), but at higher energies the experimental data points are slightly larger than the calculated yields. In Fig. 7, the actual measured electron energy distributions for 0.5 ML of oxygen on Ru(0001) are themselves shown (solid

circles), together with the energy distributions (solid lines) calculated from Eqs. (14), (6), and (7) with $A=1650$, $\gamma=1.8$, $\phi=6.2$ eV, and $k=1.60$. The fit is reasonably good, except again at the highest energies. A possible explanation of this discrepancy is that another mechanism that has an energy threshold, such as promotion of O $2s$ electrons, makes a small contribution to the electron emission in the presence of adsorbed oxygen.

A broadening of one-electron states due to a shortening of their lifetime τ, as suggested for Cl/Ru, probably also occurs on O/Ru, However, as can be shown from Eq. (11), if τ is the same for both O/Ru and Cl/Ru, the effect would manifest itself in O/Ru at a value of $1/v$ that is k times higher than for Cl/Ru. At such a higher $1/v$, the electron emission itself is weak so that deviations from the straight lines cannot be discerned in Fig. 6.

IV. CONCLUSIONS

The paper presents a study of the kinetic electron emission produced by low-energy Na^+ bombardment of Ru(0001) and Ru(0001) covered by Na, I, Cl, and O adsorbates. It is shown that the measured total electron yield and electron energy distributions can be well explained in terms of a mechanism based on nonadiabatic rapid passage of the bombarding particle through the surface interaction region. The mechanism is characterized by one parameter γ, which is the inverse value of the particle-surface effective interaction distance. A detailed microscopic description of the mechanism and of γ is not yet available, so that γ is treated as an empirical parameter and the value is deduced from experiments. As suggested by other studies, γ is less sensitive to the substrate used, but it increases with the mass of the projectile.[6] Typically, $1/\gamma$ is much smaller than the atomic radius. In fitting our experimental results, we used the same value of $\gamma=1.8$ (in a.u.) in all cases, and we changed only the work function ϕ to model changes in the electron yield that occur with surface adsorbates. The values of ϕ were obtained independently from emission thresholds, however, so that ϕ is not itself a fitting parameter.

The almost perfect agreement between the predictions of the model and the experimental data collected from clean Ru(0001) and from Ru covered with small amounts of Na and I gives credibility to the model. For very large Na coverages ($\phi=2.0$ eV), the agreement is, however, more qualitative than quantitative, and the reasons for this discrepancy are not yet understood. When Ru is covered by Cl and by O, the experimental data differ from the theoretical predictions in a systematic way which cannot be accounted for, even qualitatively, by simply using the observed changes of ϕ. Both adsorbates, particularly oxygen, introduce considerable change of the surface electronic structure because the wave functions of adsorbates are more localized and less metallic. We expect that the localization of excitations may facilitate higher-order excitation processes at the surface which cause broadening of the energy distributions. Indeed, we obtain a very good agreement with experiments by a slight broadening of the distribution using the same parameters as of clean Ru and the values of ϕ which correspond to O/Ru and Cl/Ru. The broadening for O/Ru increases the emission by 2 orders of magnitude at low impact Na^+ energies, in agreement with experiments.

We may deduce what kind of adsorbates could make the surface less metallic and thus for which adsorbates k may differ from 1. The surface electronic structure should deviate more from a metallic structure if the adsorbate provides a larger number of many-electron configurations, energetically accessible (within a few eV) in the experiments and if these configurations are made by localized electrons. If the spin degeneracy is neglected, the Na adsorbate provides only one configuration with very delocalized $3s$ electrons and we thus do not expect any nonmetallic behavior. Iodine provides three $I^0(^2P)$ and one $I^-(^1S)$ configurations of $5p$ electrons, chlorine the same four configurations with $3p$ electrons. Finally, oxygen provides nine configurations $O^0(^3P,^1D,^1S)$ and three configurations $O^-(^2P)$ with $2p$ electrons. Chlorine and iodine should behave similarly, but because chlorine $3p$ wave functions are more localized than iodine $5p$ functions, slight deviations are observed only for chlorine. The effect of surface localization is expected to be strongest, as observed experimentally, in the case of adsorbed oxygen (12 accessible configurations of $2p$ electrons) where a substantial redistribution of the electrons by higher-order electron interaction processes may occur.

The surface electron localization and many-electron aspect of the kinetic electron emission process can also explain the generally larger values of γ observed for heavier projectiles (from one-electron theory, the value of γ for Na should only be about 1 or less). For heavier projectiles, more inner-shell wave functions are mixed into the metal wave functions on the surface. The localized inner shells increase the degree of localization around the projectile at the surface and hence the electron-electron interactions, which effectively increases the value of γ.

ACKNOWLEDGMENTS

The authors wish to acknowledge National Science Foundation Grant Nos. INT-9600473 and CHE-0091328 and Czech Academical Grant No. 67801 for financial support.

*Corresponding author. FAX: 909-787-4529. Electronic address: yarmoff@ucr.edu

[1] H. D. Hagstrum, in *Inelastic Ion-Surface Collisions*, edited by N. H. Tully, J. C. Tully, W. Heiland, and C. W. White (Academic, New York, 1977), p. 1.

[2] R. Baragiola, E. V. Alonso, and A. O. Florio, Phys. Rev. B **19**, 121 (1979).

[3] B. A. Trubnikov and Y. N. Yavlinskii, Sov. Phys. JETP **21**, 167 (1965).

[4] N. Fano and W. Lichten, Phys. Rev. Lett. **14**, 627 (1965).

[5] J. A. Yarmoff, T. D. Liu, S. R. Qiu, and Z. Sroubek, Phys. Rev. Lett. **80**, 2469 (1998).

[6] J. Lorincik, Z. Sroubek, H. Eder, F. Aumayr, and H. Winter, Phys. Rev. B **62**, 16 116 (2000).

[7] J. C. Tucek, S. G. Walton, and R. L. Champion, Phys. Rev. B **53**, 14 127 (1996).
[8] W. S. Vogan, S. G. Walton, and R. L. Champion, Surf. Sci. **459**, 14 (2000).
[9] J. A. Yarmoff, H. T. Than, and Z. Sroubek, Nucl. Instrum. Methods Phys. Res. A (to be published).
[10] J. C. Tucek and R. L. Champion, Surf. Sci. **382**, 137 (1997).
[11] L. Surnev, G. Rangelov, E. Bertel, and F. P. Netzer, Surf. Sci. **184**, 10 (1987).
[12] L. Surnev, G. Rangelov, and G. Bliznakov, Surf. Sci. **159**, 299 (1985).
[13] N. D. Spencer, P. J. Goddard, P. W. Davies, M. Kitson, and R. M. Lambert, J. Vac. Sci. Technol. A **1**, 1554 (1983).
[14] *Physics of Solid Surfaces*, edited by G. Chiarotti, Landolt-Börnstein, New Series, Group III, Vol. 24b (Springer, Berlin, 1994).
[15] J. B. Marston, D. R. Andersson, E. R. Behringer, and B. H. Cooper, Phys. Rev. B **48**, 7809 (1993).
[16] T. L. Ferrell and R. H. Ritchie, Phys. Rev. B **16**, 115 (1977).
[17] G. Falcone and Z. Sroubek, Phys. Rev. B **39**, 1999 (1989).
[18] Z. Miskovic, J. Vukanic, and T. E. Madey, Surf. Sci. **141**, 285 (1984).
[19] G. Rangelov and L. Surnev, Surf. Sci. **185**, 457 (1987).
[20] S. Pülm, A. Hitzke, J. Günster, W. Maus-Friedrichs, and V. Kempter, Surf. Sci. **325**, 75 (1995).
[21] N. J. Gudde and R. M. Lambert, Surf. Sci. **134**, 703 (1983).
[22] I. Pollini, Phys. Rev. B **50**, 2095 (1994).